

Published in final edited form as:

Biochemistry. 2013 November 19; 52(46): . doi:10.1021/bi401188w.

## Thermodynamic Analysis of Transition State Features in Picomolar Inhibitors of Human 5' Methylthioadenosine Phosphorylase

Rong Guan<sup>‡</sup>, Peter C. Tyler<sup>§</sup>, Gary B. Evans<sup>§</sup>, and Vern L. Schramm<sup>\*,‡</sup>

<sup>‡</sup>Department of Biochemistry, Albert Einstein College of Medicine, Yeshiva University, 1300 Morris Park Avenue, Bronx, NY 10461, USA <sup>§</sup>Carbohydrate Chemistry, Callaghan Innovation, Ltd., Lower Hutt, New Zealand.

### Abstract

Human 5'-methylthioadenosine phosphorylase (MTAP) is solely responsible for 5'-methylthioadenosine (MTA) metabolism to permit S-adenosylmethionine salvage. Transition state (TS) analogues of MTAP are in development as anticancer candidates. TS analogues of MTAP incorporate a cationic nitrogen and a protonated 9-deazaadenine leaving group, mimics of the ribocation transition state. MT-ImmA and MT-DADMe-ImmA are two examples of these TS analogues. Thermodynamic analysis of MTA, inhibitor and phosphate binding reveals the cationic nitrogen to provide  $-2.6$  and  $-3.6$  kcal/mol binding free energy for MT-ImmA and MT-DADMe-ImmA, respectively. The protonated deazaadenine provides an additional  $-1.3$  (MT-ImmA) to  $-1.7$  kcal/mol (MT-DADMe-ImmA). MT-DADMe-ImmA is a better match in TS geometry than MT-ImmA and is thermodynamically favored. Binding of TS analogues to the MTAP:phosphate complex is fully entropic, in contrast to TS analogue binding to the related human purine nucleoside phosphorylase:phosphate complex, which is fully enthalpic. The binding thermodynamics of phosphate or TS analogues alone to MTAP are fully dominated by enthalpy. Phosphate anchored in the catalytic site forms an ion pair with the cationic TS analogue to cause stabilization of the enzyme structure in the ternary complex. The ternary-induced conformational changes convert the individual enthalpic binding energies to entropy, a presumed shift of the protein architecture toward the transition state. Formation of the ternary TS analogue complex with MTAP induces a remarkable increase in thermal stability ( $\Delta T_m$  35 °C). The enthalpic, entropic and protein stability features of TS analogue binding to human MTAP are resolved in these studies.

### Keywords

transition state analogues; MTAP; binding energy; thermodynamics; cooperativity; protein stabilization; entropic binding

The metabolite 5'-methylthioadenosine (MTA) links the polyamine biosynthesis and S-adenosyl-L-methionine (SAM) recycling pathways. MTA in humans is produced exclusively from decarboxy-SAM during the biosynthesis of spermine and spermidine.<sup>1</sup> MTA is metabolized only through the phosphorolysis catalyzed by 5'-methylthioadenosine phosphorylase (MTAP) to adenine and 5-methylthioribose-1-phosphate. Adenine is recycled

\* To whom correspondence should be addressed. Telephone: +1 718 430 2813. Fax: +1 718 430 8565. vern.schramm@einstein.yu.edu..

to the adenylate pool via adenine phosphoribosyltransferase and 5-methylthioribose-1-phosphate is recycled to methionine, precursors of SAM recycling.<sup>2,3</sup> There is no significant MTA in normal mammalian tissues, but inhibition of MTAP in mice causes accumulation of MTA in blood and urine and in rare human deficiencies of MTAP, MTA is also found in the blood.<sup>4-6</sup> Although the metabolic effects of MTA accumulation are incompletely understood, feedback inhibition of polyamine biosynthesis and inhibition of SAM salvage from MTA have been proposed.<sup>4</sup> Altered SAM pools are then proposed to influence epigenetic control via protein and DNA methylations, and thus inhibit proliferation of cancer cells.<sup>4</sup> The unique role of human MTAP (*MTAP*) in MTA metabolism supports its significance as an anticancer target.<sup>4,5</sup>

Transition state analysis for *MTAP* used kinetic isotope effects and quantum computational chemistry to aid in the design of transition state (TS) analogue inhibitors.<sup>7</sup> A late dissociative transition state was proposed to include a cationic ribosyl anomeric carbon and an anionic leaving group (Figure 1A).<sup>7</sup> Based on this transition state structure, two generations of TS analogue inhibitors were synthesized, but with N7 protonated to mimic the anionic N7 stabilized by hydrogen bonding with a proton of Asp220 at the transition state. Analogues with similarity to the TS exhibited high binding affinity to the *MTAP*:phosphate complex.<sup>8-10</sup> MT-ImmA and MT-DADMe-ImmA are examples of first and second generation TS analogues for *MTAP*, with dissociation constants of 1 nM and 90 pM, respectively. Substitutions for the 5'-methylthio group can increase the affinity, thus the  $K_d$  for pCIPhT-DADMe-ImmA is 10 pM (Figure 1B).<sup>9,10</sup> These inhibitors possess transition state features with a cationic nitrogen mimicking the cationic anomeric carbon and the 9-deazaadenine mimicking the adenine leaving group. MT-ImmA has only a single C-N bond distance (1.5 Å) between the cationic nitrogen and the leaving group, resembling a substrate-like early transition state. MT-DADMe-ImmA increases that distance to 2.8 Å through incorporation of a methylene bridge, to more accurately reflect the geometry of the late dissociative transition state and hence shows the tighter binding affinity. In immunodeficient mice, treatment with MT-DADMe-ImmA causes remission of human head and neck cancer, and suppresses the growth and metastases of human lung cancer.<sup>4,5</sup> The high efficacy and low toxicity of MT-DADMe-ImmA suggests potential as a new approach for cancer treatment.

Isothermal titration calorimetry (ITC) studies were used earlier to explore the tight binding of transition state analogues to the *MTAP*:phosphate complex.<sup>11</sup> The analysis revealed an unexpected thermodynamic signature with favorable entropy but unfavorable enthalpy upon formation of the ternary TS analogue complex. *MTAP* and its homologous enzyme, human purine nucleoside phosphorylase (*HsPNP*), share similar overall structures and related TS analogue inhibitors.<sup>12,13</sup> Both enzymes are homotrimers with three active sites located near the subunit interfaces. The enzymes differ in catalytic site cooperativity. Filling a single catalytic site of *HsPNP* fully inhibits the enzyme while all three sites of *MTAP* must be filled with TS analogues to cause complete inhibition.<sup>11,14</sup> Binding of TS analogues to the *HsPNP*:phosphate complex is driven by a favorable enthalpy with entropic penalties, exactly opposite to the thermodynamic signature for *MTAP*.<sup>11,13</sup> The entropically-driven binding of transition state analogues to *MTAP* was surprising because the crystal structures of *HsPNP* and *MTAP* with transition state analogues show similar hydrogen bond and ionic bond interactions but opposite thermodynamic patterns. The pattern with *MTAP* suggested an increased order in the enzyme active site and the overall protein structure, to cause the release of water from the subunit interfaces and especially from the active site.<sup>11</sup> The most significant conformational change was observed for a loop of nine amino acid residues 227 to 235, which is flexible in the apo enzyme but is ordered in the ternary TS analogue complexes.<sup>11</sup> The ordered loop blocks the solvent channel to the enzyme active site and expels the water inside, consistent with the observed entropic binding. The distinct

thermodynamic signatures of *MTAP* and *HsPNP* for binding to their transition state analogues suggest that even closely related enzymes have specifically evolved mechanisms of converting substrates to the transition state.<sup>11</sup>

Previous thermodynamic studies of *MTAP* focused on the formation of the ternary TS analogue complex.<sup>11</sup> Here we dissect the binding of individual phosphate and TS analogue components to the apo enzyme and subsequent formation of the ternary complex. The binding thermodynamics of each component is explored to provide full thermodynamic cycles for TS analogue binding. Contributions to binding free energy are derived from thermodynamic cycles for both generations of TS analogues. Thermodynamic signatures are also determined for each component with evaluation and corrections for the protonation effects on binding, and are evaluated in terms of the entropic-driving force for formation of the complexes proposed to be related to the functional TS complex. Finally, we experimentally verify that the ternary complex with bound TS analogue is highly stabilized to heat denaturation. Thus, the entropically driven formation of the ternary complex reflects solvent reorganization and not protein destabilization toward a denatured state. This work provides insights into the thermodynamic nature of TS analogue interactions with *MTAP*. The unique mechanisms of converting binding enthalpy to entropy provide a general lesson on TS analogue interactions with their targets.

## MATERIALS AND METHODS

### Chemicals

MT-ImmA and MT-DADMe-ImmA were synthesized as described elsewhere.<sup>9,10</sup> MTA and potassium phosphate were purchased from Sigma. All other chemicals and reagents were obtained from either Sigma or Fisher Scientific and were of the highest grades of purity available.

### Enzyme Preparation

The purification of human *MTAP* has been detailed previously.<sup>12</sup> Briefly, a plasmid containing the synthetic gene of *MTAP* was transformed into BL21-CodonPlus(DE3)-RIPL *E. coli* cell. Cells were grown at 37 °C in LB medium containing 100 µg/mL ampicillin and induced by addition of 1 mM IPTG (final concentration). Cells were collected and disrupted by French Press. The supernatant was loaded onto a Ni-NTA superflow column for purification. *MTAP* was eluted with a buffer containing 50 mM phosphate, 300 mM NaCl, and 80 mM imidazole, at pH 8.0. Purified enzyme was dialyzed against 100 mM phosphate, pH 7.4 with 5 mM DTT and stored at –80 °C. Recombinant *MTAP* contains 14 additional amino acids at the N-terminus, including a His<sub>6</sub> tag, and is catalytically equivalent to the native enzyme. The additional N-terminal residues are far away from the active site and are disordered in the crystal structures.<sup>12</sup> The expressed form of human *MTAP* has an estimated extinction coefficient of 30.94 mM<sup>–1</sup>cm<sup>–1</sup> at 280 nm, the constant used to estimate protein concentrations (ProtParam program from ExPASy).

### Isothermal Titration Calorimetry Studies

Purified *MTAP* exists as homotrimer and as purified above, approximately two-third of the active sites are occupied by its product, adenine. Co-purified adenine was removed by dialyzing the enzyme against 0.5% (V/V) charcoal in 100 mM phosphate, pH 7.4 for 3 hours.<sup>12</sup> Adenine-free *MTAP* was further dialyzed against a buffer containing 50 mM Hepes and 100 mM NaCl at pH 7.4, with at least three buffer changes to obtain apo enzyme free of bound phosphate. ITC studies were performed on a VP-ITC MicroCalorimeter. Dialysate and apo *MTAP* were filtered (Millipore, 0.2 µm) right before experiments. The filtered dialysate was used as solvent to prepare the ligand solutions. *MTAP* sample (40 µM) and

ligand solution (600  $\mu\text{M}$ ) were degassed (Microcal Thermovac) for 15 minutes and loaded into a 1.46 mL sample cell and 250  $\mu\text{L}$  injection syringe of the calorimeter, respectively. Isothermal titrations included 20-30 injections of 4-6  $\mu\text{L}$  inhibitor solutions, with a spacing of 230 s between injections. Human *MTAP* slowly hydrolyzed MTA in the absence of phosphate with a  $k_{\text{cat}}$  of  $(5.1 \pm 0.1) \times 10^{-5} \text{ s}^{-1}$  as estimated by UPLC. To avoid significant hydrolysis of MTA, ITC experiments for MTA used a low concentration of enzyme (25  $\mu\text{M}$ ) and MTA (350  $\mu\text{M}$ ) with 18 injections at 9  $\mu\text{L}$ /injection and a shorter interval time of 180 s. To explore the protonation/deprotonation effect on the binding of inhibitors and phosphate, ITC studies were carried out in a buffer (50 mM Tris and 100 mM NaCl at pH 7.4) with a different ionization enthalpy from the HEPES buffer. Other experimental conditions were kept the same as described above. Isothermal titrations were at 25  $^{\circ}\text{C}$  and were initiated with adenine-free and phosphate-free apo enzyme. Heat of dilution corrections were added from control experiments by titrating the ligand into buffer.

### ITC Data Processing

ITC data of MT-ImmA (first generation inhibitor) and phosphate titrations gave the best results when fitted to the single set of identical sites model. Data of MT-DADMe-ImmA (second generation inhibitor) and MTA binding fit the best to a model for two sets of independent sites. Dissociation constants ( $K_{\text{d}}$ ) for those ligands were determined from the ITC-data fitting.  $\Delta G$  values were calculated from  $K_{\text{d}}$  using equation 1. The entropy terms ( $-T\Delta S$ ) were calculated from equation 2 (the Gibbs free energy expression).

$$\Delta G = RT \ln K_{\text{d}} \quad (1)$$

$$\Delta G = \Delta H - T\Delta S \quad (2)$$

Equations 3 and 4 represent the total heat content of the solution ( $Q$ ) contained in the active cell volume ( $V_0$ ) for a single set of identical sites and two sets of independent sites, respectively. Equation 5 represents the heat released ( $\Delta Q_i$ ) from the  $i$ th injection in an ITC experiment. In equations 3-5,  $n$  is the number of sites,  $\Theta$  is the fraction of sites occupied by ligand,  $dV_i$  is the injection volume,  $M_t$  is the concentration of the protein in  $V_0$ , and  $\Delta H$  is the molar heat from inhibitor binding. ITC data were fitted using software Origin 7.0 and followed the same procedures for single set of identical sites and two sets of independent sites models. Initial guesses of  $n$ ,  $K_{\text{a}}^1$  and  $\Delta H$  were generated by the algorithm.  $\Delta Q_i$  for each injection was calculated and compared with the corresponding heat obtained from experiment. The values of  $n$ ,  $K_{\text{a}}$  and  $\Delta H$  were optimized using standard Marquardt methods and iterated to reach the best fit to the model. The  $n$  value has been determined to be 3 for human *MTAP* and was directly input into Origin 7.0 for accurate fitting (12). More details of the data processing are available on the User's Manual for VP-ITC MicroCalorimeter.

$$Q = n\Theta M_t \Delta H V_0 \quad (3)$$

$$Q = M_t V_0 (n_1 \Theta_1 \Delta H_1 + n_2 \Theta_2 \Delta H_2) \quad (4)$$

$$\Delta Q_i = Q_i + \frac{dV_i}{V_0} \left( \frac{Q_i + Q_{i-1}}{2} \right) - Q_{i-1} \quad (5)$$

<sup>1</sup> $K_{\text{a}}$  is the association constant of ligand, the reciprocal of dissociation constant  $K_{\text{d}}$ .  $K_{\text{i}}$  is the dissociation constant of inhibitors.

## Differential Scanning Fluorimetry Studies

A 7900HT Fast Real-Time PCR System was used to conduct the differential temperature scanning fluorimetry experiments of *MTAP*. Samples of 10  $\mu$ L were monitored in wells of a 384-well plate with 10 replicates for each condition, containing 50 mM Hepes (pH 7.4), 100 mM NaCl, 25  $\mu$ M *MTAP*, 1X Sypro Orange (from vendor solution), 0 or 20 mM phosphate, and 0 or 500  $\mu$ M TS analogues. A control was included without enzyme, phosphate or TS analogues. The melting temperatures ( $T_m$  values) were determined as described earlier by using GraFit 5 (Erithacus Software) and the Boltzmann equation.<sup>16</sup>

## RESULTS AND DISCUSSION

MT-ImmA and MT-DADMe-ImmA possess a cationic nitrogen and protonated N7 to mimic two main TS features of *MTAP* (Fig. 1). MT-ImmA represents the substrate-like early transition state with a 1.5 Å single C-N bond between the cationic ribosyl mimic and the leaving group. MT-DADMe-ImmA extends the distance to 2.8 Å with a methylene group insertion, a mimic of a late transition state geometry. Thermodynamics of TS analogue inhibitor binding to the *MTAP*:phosphate complex is entropically driven, but the thermodynamics of binding phosphate and TS analogue to the apo *MTAP* are needed to understand the binding order, cooperativity of binding and the thermodynamic cycle. ITC studies were carried out for binding of MT-ImmA, MT-DADMe-ImmA, phosphate, and MTA to apo *MTAP* in Hepes buffer to resolve the complete thermodynamic cycles for the binding of both generations of inhibitors. Analysis of the thermodynamic cycles provides estimates of the thermodynamic contributions from the cationic nitrogen upon inhibitor binding. The comparison of binding free energy for MTA relative to the TS analogues also provides an estimation of thermodynamic contributions from the 9-deazaadenine group.

### Affinity and Binding Free Energy of Ligands to apo *MTAP*

The dissociation constants and binding free energy of ligands to apo *MTAP* were obtained from ITC experiments in Hepes buffer (Table 1 and Figure 2). MT-ImmA binds to apo *MTAP* tightly with a  $K_d$  of 70 nM and a free binding energy of  $-9.7$  kcal/mol for the three active sites of the trimeric enzyme, showing no binding cooperativity. MT-DADMe-ImmA binds even tighter in the first two sites with a  $K_d$  of 40 nM and a  $\Delta G$  of  $-10.1$  kcal/mol. The dissociation constant of the third site decreased to 110 nM, suggesting modest negative cooperativity for binding at the third site. The  $K_d$  of phosphate is 17  $\mu$ M for all three sites with a  $\Delta G$  of  $-6.51$  kcal/mol. Binding of the substrate MTA exhibits a  $K_d$  of 8 nM for the first site but 700 nM for the latter two sites, exhibiting significant negative cooperativity. Steady-state kinetic analysis gives a  $K_m$  of 1.7  $\mu$ M for MTA with a significant forward commitment, consistent with a  $K_d$  of 700 nM but not 8 nM, thus the effects of phosphate binding substantially alter the MTA binding parameters.<sup>7,12</sup> *MTAP* slowly hydrolyzes MTA in the absence of phosphate with a  $k_{cat}$  of  $5.1 \times 10^{-5} \text{ s}^{-1}$ . This slow reaction does not affect the ITC experiments under our selected experimental conditions. However, the hydrolytic reaction reinforces the dissociative catalytic mechanism of *MTAP*, showing formation of the ribocationic transition state with weak participation of the phosphate nucleophile. The *MTAP*:MTA complexes are capable of reaching the transition state without phosphate, albeit with a higher barrier than with phosphate.

Previous studies have shown that the binding of TS analogue inhibitors to the *MTAP*:phosphate complex is completely driven by entropy, interpreted as the result of protein contraction and exclusion of water from the active site and the protein trimeric interfaces.<sup>12</sup> The entropic term ( $-T\Delta S$ ) for MTA binding to the first (tight) site is  $-10.1$  kcal/mol, dominating the  $\Delta G$  of  $-11.1$  kcal/mol. This thermodynamic pattern is distinct from the binding of other ligands to apo *MTAP* and to the binding of MTA to the remaining two sites,



but is consistent with the binding of TS analogues to the *MTAP*:phosphate complex (Table 1). In the first site, MTA forms a ternary complex with water and *MTAP*, and achieves a tight binding affinity by the complex ability to acquire some part of the transition state characteristic. Tightly bound MTA at the first site alters the conformation of the neighboring two subunits to decrease the affinity for the next sites. The  $K_d$  values of 700 nM for the latter two sites are similar to the steady-state kinetic parameter for  $K_m$ , but the  $K_m$  also represents contributions from interaction with phosphate.

### Thermodynamic Cycles of binding TS Analogue Inhibitors

ITC studies on ligands binding to apo enzyme were combined with studies of TS analogues binding to the *MTAP*:phosphate complex, allowing the construction of thermodynamic cycles for each component of binding in forming the ternary complex with TS analogues (Figures 4 & 5). The ternary TS analogue complex can be obtained through two binding routes provided that random binding is possible. ITC demonstrates that either phosphate or inhibitor can bind first, followed by the second ligand.  $\Delta G$  is a state function and dependent only on the initial and final states but not the path taken in the cycle. Therefore,  $\Delta G_1 + \Delta G_2 = \Delta G_3 + \Delta G_4$  (Figures 4 & 5). At fixed temperature,  $\Delta G$  is a function of the dissociation constant, defined as  $RT \ln K_d$ . Thus, the dissociation constants follow the relationship:  $K_{d1} \times K_{d2} = K_{d3} \times K_{d4}$ . The  $\Delta G$  and  $K_d$  values for binding phosphate to the *MTAP*:inhibitor complex are derived from these equations. The  $\Delta \Delta G$  is calculated from  $\Delta G_2 - \Delta G_3$ , representing the coupling free energy for the interactions between phosphate and the TS analogues. Since the interactions are mainly contributed by the cationic nitrogen-phosphate ion pair,  $\Delta \Delta G$  value provides the thermodynamic contributions from the cationic nitrogen of the TS analogue.

The crystal structure of *MTAP* in complex with phosphate and MT-ImmA shows interactions between phosphate and MT-ImmA to include two hydrogen bonds to the 2'- and 3'-hydroxyl groups of the inhibitor and an ion pair between phosphate and the cationic nitrogen.<sup>5</sup> The phosphate-specific interactions contribute a  $\Delta \Delta G$  value of -2.6 kcal/mol and increase the affinity of MT-ImmA from 70 nM without phosphate to 1 nM in the ternary complex. The crystal structure of *MTAP* in complex with phosphate and pClPhT-DADMe-ImmA shows a single phosphate:inhibitor interaction, the ion pair between phosphate and the cationic nitrogen.<sup>12</sup> pClPhT-DADMe-ImmA and MT-DADMe-ImmA both belong to the second generation of ImmAs with the only difference being the remote 5'-methylthio substituent. Therefore, they are expected to exhibit the same contacts with phosphate. The single ion pair in the complex of *MTAP*:phosphate:MT-DADMe-ImmA is estimated to exhibit a  $\Delta \Delta G$  value of -3.6 kcal/mol, more favorable than the -2.6 kcal/mol  $\Delta \Delta G$  from three interactions formed to MT-ImmA, including an ion pair formed by same cationic nitrogen and phosphate. This energy difference indicates that the cationic nitrogen of MT-DADMe-ImmA is better positioned to form a thermodynamic favored ion pair and supports the proposal that MT-DADMe-ImmA more accurately resembles the enzymatic transition state. Optimal TS analogues must capture both the geometry and the charges at the transition state to achieve the highest binding affinity. In this case, the extra binding free energy decreases the  $K_d$  of MT-DADMe-ImmA 440-fold, from 40 nM to 90 pM.

The thermodynamic cycles reveal that the *MTAP*:inhibitor complexes bind phosphate tighter than the apo enzyme, thus bound inhibitors provide optimization of the phosphate binding site. Thus, phosphate and TS analogue free energy of binding is synergistic independent of which is bound first. In terms of a physiological interpretation of how TS analogues will interact with *MTAP*, with a  $K_d$  for phosphate of only 17  $\mu$ M, much lower than the mM phosphate concentration of cells, the inhibitor would primarily bind to *MTAP*:phosphate complexes rather than the apo *MTAP*.

## Thermodynamic Contributions from the 9-Deazaadenine of TS Analogues

The natural substrate MTA is unprotonated at N7 but transition state analogue inhibitors have the N7 protonated. Crystal structures of *MTAP* in complex with MTA or MT-ImmA suggest that the interactions between enzyme and these catalytic site ligands are nearly identical except for the hydrogen bond formed between Asp220 and N7. Asp220 is anticipated to be anionic for hydrogen bonding to the N7 of the deazaadenine but neutral for hydrogen bonding to the N7 of adenine. Transition state analysis suggests an anionic leaving group at the *MTAP* transition state, but with H-bond formation to N7 by Asp220, thus the transition state analogue gains thermodynamic advantage from N7 hydrogen bond formation with Asp220.<sup>7</sup> The *MTAP* structure in complex with pCIPhT-DADMe-ImmA has the same set of interactions between 9-deazaadenine group and enzyme as the MT-ImmA structure, and is not influenced by the relatively large 5'-pCIPh-group or the 2'-deoxy-,<sup>5,12</sup> predicting the same interactions at the N7 for MT-DADMe-ImmA. Both pCIPhT-DADMe-ImmA and MT-DADMe-ImmA are missing the 2'-OH group, which forms a hydrogen bond with the peptide backbone of residue Met196. Therefore, the binding of MT-DADMe-ImmA to *MTAP* is different from that of MTA in two aspects: an altered  $pK_a$  at N7 for optimal hydrogen bonding to Asp220 and one less hydrogen bond with Met196. There are no nearby interactions between the cationic nitrogen of inhibitors or the C4' oxygen of MTA to the enzyme. Therefore, the cationic nitrogen features of TS analogues are not directly involved in ligand contacts to the apo enzyme. It is, however, possible that the presence of the cationic nitrogen in transition state analogues could cause remote electrostatic interactions not detected in crystal structures.

The binding free energy of MTA, MT-ImmA, and MT-DADMe-ImmA to apo *MTAP* allows the estimation of thermodynamic contributions from the 9-deazaadenine ring, which are reflected in the  $\Delta\Delta G$  values calculated by subtracting the binding free energy of MTA from those of inhibitors (Figure 6). MT-ImmA has a  $\Delta\Delta G$  value of  $-1.3$  kcal/mol relative to MTA, attributed to the 9-deazaadenine feature of altered  $pK_a$  at N7. A  $\Delta\Delta G$  value of  $-1.7$  kcal/mol is determined for MT-DADMe-ImmA, suggesting that the thermodynamic advantage from the 9-deazaadenine feature overcomes the disadvantage of losing the 2'-OH hydrogen bond, and improves the binding free energy to the enzyme compared to MT-ImmA. First and second generations of TS analogues possess the same 9-deazaadenine leaving group with elevated  $pK_a$  at N7 but the second generation inhibitor, MT-DADMe-ImmA, gains more thermodynamic advantage from the feature, emphasizing the importance of appropriate geometry of the transition state analogue.

## Protonation/deprotonation effects on thermodynamic parameters

The binding of ligands to protein may couple to the release or absorption of protons from the binding complex. In solution, the protons exchange with buffer to cause an ionization enthalpy. The protonation/deprotonation effects can be evaluated by performing the same ITC experiments in two buffers with different ionization enthalpies, a documented technique.<sup>15</sup> In this study, Hepes and Tris buffers were chosen with ionization enthalpies of 4.876 and 11.341 kcal/mol, respectively. Thus, proton release from the *MTAP*:ligand complex will cause an additional enthalpy change of  $-6.465$  kcal/mol for  $\Delta H_{\text{Tris}} - \Delta H_{\text{Hepes}}$ .<sup>16</sup> The differential  $\Delta H$  values can be used to estimate the number of protons exchanged with buffer and to correct the protonation/deprotonation effects on the  $\Delta H$  values of ligands ( $\Delta H_{\text{correction}}$ ) (Table 2).

The dissociation constants of ligands obtained from ITC experiments in Hepes were used for the fitting of the ITC data from Tris buffer. Binding enthalpies for MT-ImmA, MT-DADMe-ImmA, and phosphate were affected by the buffer selection (Figure 3). Thus the binding enthalpy for those ligands allows analysis of the protonation/deprotonation effects.

The binding of MT-ImmA to apo *MTAP* releases 0.5 protons into the buffer solution. MT-DADMe-ImmA binding releases 0.2 protons for the binding to the first two sites of trimeric *MTAP* but 1.1 protons for the binding of the third site, suggesting different catalytic site ionizations between the first two and the third sites upon binding, consistent with the negative binding cooperativity observed in the isothermal titrations (Figures 2 & 3). At pH 7.4, 80% of the phosphates are dibasic. ITC data indicates that phosphate binds to apo *MTAP* with absorption of  $0.91 \pm 0.05$  protons from the buffer, implicating monobasic bound phosphate or that an enzyme group becomes protonated upon dibasic phosphate binding.

The corrected  $\Delta H$  ( $\Delta H_{\text{correction}}$ ) and  $-T\Delta S$  ( $-T\Delta S_{\text{correction}}$ ) values are the binding enthalpy and entropy without protonation or deprotonation effects, representing the intrinsic thermodynamic signatures of ligand binding (Table 2 & Figure 7). Previous studies revealed that binding of TS analogues to *MTAP*:phosphate is completely driven by entropy with an enthalpic penalty. This observation was explained by the closing of enzyme active site and overall compacting of the trimeric structure, to cause exclusion of water from the active site and subunit interfaces, and thereby dominate the entropy term. In contrast, the binding of individual phosphate and TS analogues to apo *MTAP* shows distinct thermodynamic signatures with enthalpy as the major contributor. MT-ImmA and MT-DADMe-ImmA bind to apo *MTAP* with a  $\Delta H_{\text{correction}}$  of  $-7.15$  and  $-9.2$  kcal/mol, respectively, accounting for 74% and 91% of total binding free energy for each inhibitor. The  $\Delta H_{\text{correction}}$  of phosphate is  $-13.1$  kcal/mol and it pays a strong entropic penalty of 6.6 kcal/mol. Phosphate and transition state analogues all bind enthalpically, reflecting the formation of favorable hydrogen or ionic bonds but a still opened enzyme active site. The large entropic penalty on phosphate binding suggests a loss of dynamic structure surrounding the phosphate binding site upon binding. The results indicate that it is the interaction between phosphate and TS analogue that closes the active site, expels water, and converts binding enthalpy to entropy. Crystal structures of apo *MTAP* and *MTAP* in complex with TS analogues and phosphate have revealed that the binding of phosphate caused no significant conformational changes to the *MTAP* structures but the binding of TS analogues causes the closure of the active site by the motion of a loop (residue 227-235) which is flexible in the apo enzyme but closed in the complexes.<sup>12</sup> The overlaid structures of *MTAP* in complex with adenine (PDB ID: 1CB0) and in complex with phosphate and MT-ImmA (PDB ID: 1K27) show the inhibitor MT-ImmA is pulled toward the phosphate with a more ordered loop of residues 227 to 235 (Figure 8). Phosphate is the anchor for the TS analogues and their ion pair formation provides the driving force to cause the active site to close. Although the protein is proposed to become more organized (less dynamic), normally an entropic penalty, the altered water access to the protein is proposed to dominate for a net entropic driving force for the closed complex.

### Testing *MTAP* Stability in the Ternary Complexes

Thermodynamic data for *MTAP* revealed that the overall binding of inhibitors was driven by favorable entropy, supporting a more disordered state. However we propose that the ternary complexes are more thermodynamically stable than apo *MTAP* or binary complexes based on the unique enthalpy-entropy converting mechanism of this enzyme at its transition state. Our hypothesis was tested using differential temperature scanning fluorimetry. Apo *MTAP* gave a  $T_m$  of 67.1 °C and the binary complex with phosphate decreased stability slightly to 65.7 °C (Figure 9). Binding of MT-ImmA or MT-DADMe-ImmA in binary or ternary complexes showed a remarkable ability to stabilize the protein with  $T_m$  values of 95.1 to 95.6 °C for all complexes with TS analogues. Thus, the entropic contributions found in the ternary TS complexes are not on the path to dynamic unfolding, but induce extraordinary thermal stability. This finding is consistent with structural and heat capacity changes that



reported altered hydrophobic interactions and release of water upon binding of TS analogues to *MTAP*.<sup>11</sup>

## Conclusions

*MTAP* catalyzes the phosphorolysis of MTA and requires the simultaneous binding of MTA and phosphate to generate the transition state. The enzyme binds phosphate and TS analogues independently to form stable, enthalpy-driven binary interactions. Formation of the ternary complex with enzyme, TS analogue and phosphate causes a large, favorable entropic change reflecting a conformational change in the protein that excludes water from the catalytic site and subunit interfaces of the protein. The driving force for formation of the entropically favorable ternary complex is an enzyme-bound ion pair between the anionic phosphate and cationic transition state analogues. Binary *MTAP*:TS analogue or ternary *MTAP*:TS analogue:phosphate complexes demonstrate remarkable thermal stability with a  $T_m$  near 95 °C, a  $\Delta T_m$  of 28 °C compared to apo *MTAP*.

The substrate MTA shows a binding pattern distinct from the TS analogues. It binds tightly to the first catalytic site, driven by a large and favorable entropy, and binds less tightly to the 2<sup>nd</sup> and 3<sup>rd</sup> sites, driven by enthalpy, similar to the binary complexes with phosphate or TS analogues. MTA binding is reminiscent of adenine binding to *MTAP*:phosphate by also showing negative cooperativity and is entropy-driven, suggesting that adenine interactions dominate the first-site MTA interaction, and alters binding thermodynamics at the remaining two sites.<sup>11</sup>

TS analogue binding is favored by the elevated  $pK_a$  of N7 in 9-deazaadenine, and the cationic nitrogen mimic of the ribocation at the TS. Thus, MT-ImmA binds 1,700 times and MT-DADMe-ImmA binds 18,900 times tighter than the  $K_m$  for MTA.

ITC studies provided the thermodynamic parameters for phosphate, MTA and TS analogue inhibitors to *MTAP*. The use of two buffer systems provided estimates of proton release or uptake for the interactions of TS analogues and phosphate.

Thermodynamic characterization of *MTAP* reveals a unique mechanism of enthalpically favorable binding of phosphate and nucleoside components but using that energy in a conformational reorganization with favorable entropic characteristics to deliver the bound reactants toward the transition state. This reorganization is revealed by quantitating the conversion of binding enthalpy to entropy in tight complexes with TS analogues.

## Acknowledgments

Funding. This work was supported by NIH research grants GM41916 and CA135405.

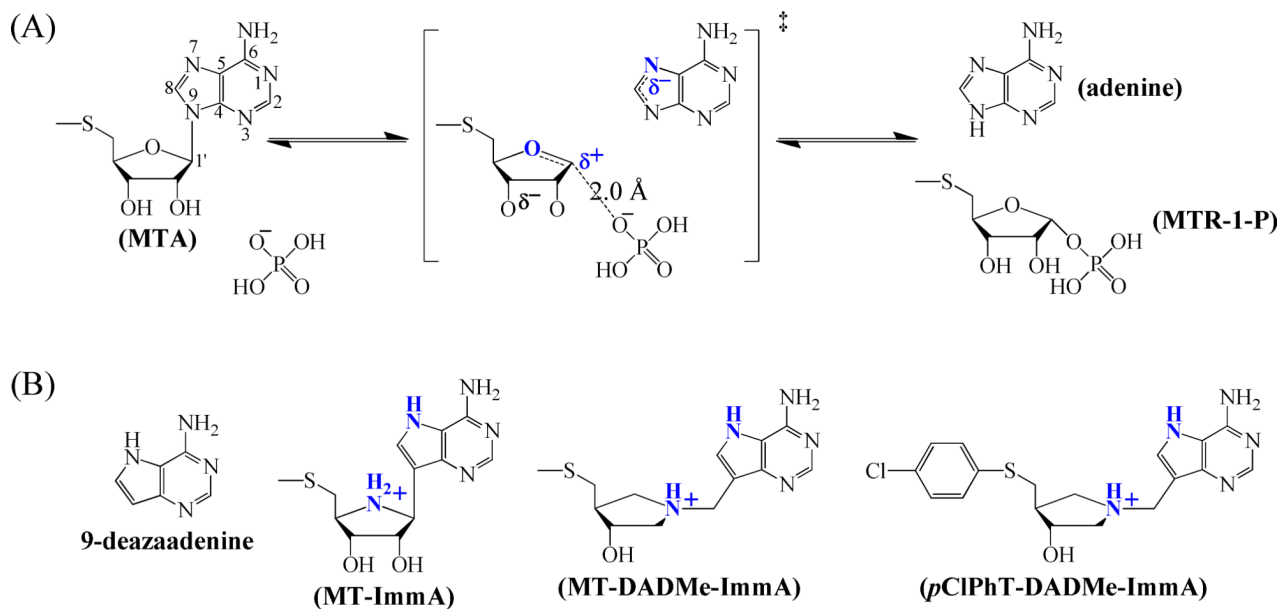
## Abbreviations

<b>MTA</b>	5'-methylthioadenosine
<b>SAM</b>	S-adenosyl-L-methionine
<b>MTAP</b>	MTA phosphorylase
<b>PNP</b>	purine nucleoside phosphorylase
<b>MTR-1-P</b>	5-methylthioribose- $\alpha$ -D-1-phosphate
<b>ImmA</b>	Immucillin-A
<b>DADMe</b>	4'-deaza-1'-aza-2'-deoxy-1'-(9-methylene)

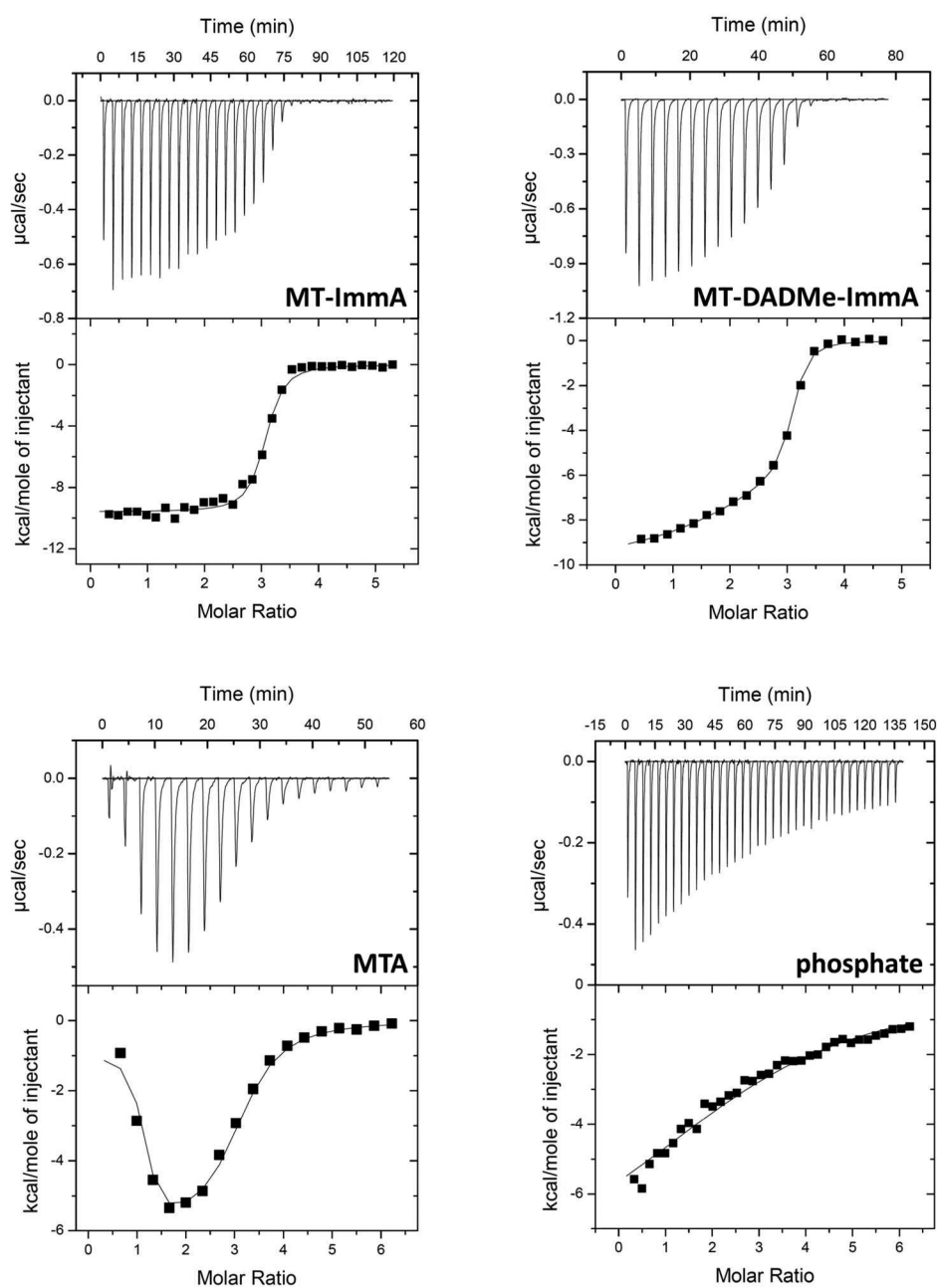
TS transition state

## REFERENCES

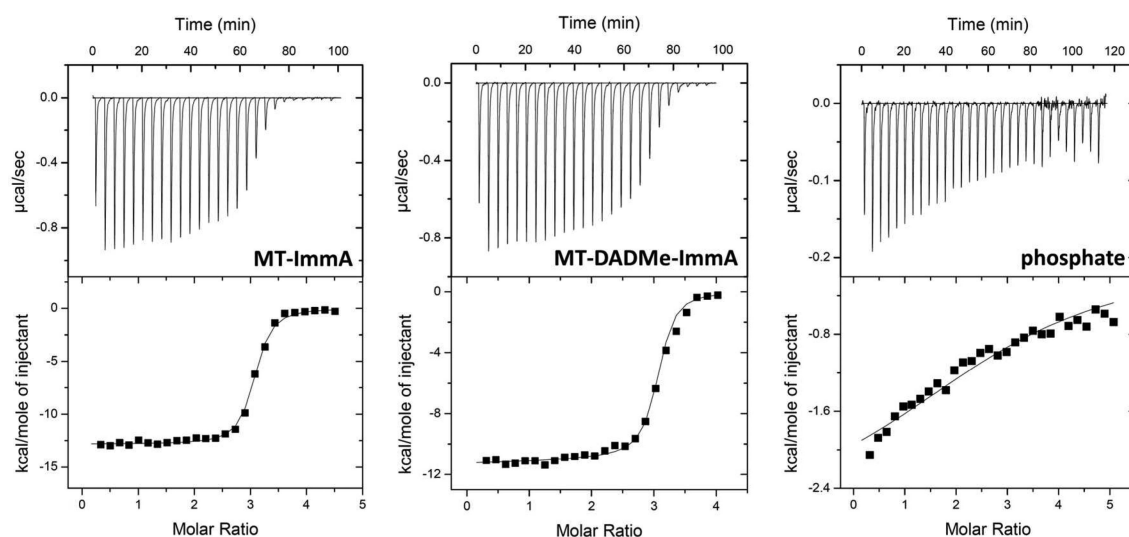
1. Williams-Ashman HG, Seidenfeld J, Galletti P. Trends in the biochemical pharmacology of 5'-deoxy-5'-methylthioadenosine. *Biochem. Pharmacol.* 1982; 31:277–288. [PubMed: 6803807]
2. Cacciapuoti G, Oliva A, Zappia V. Studies on phosphate-activated 5'-methylthioadenosine nucleosidase from human placenta. *Int. J. Biochem.* 1978; 9:35–41. [PubMed: 631411]
3. Kamatani N, Carson DA. Dependence of adenine production upon polyamine synthesis in cultured human lymphoblasts. *Biochimica et Biophysica Acta, General Subjects.* 1981; 675:344–350.
4. Basu I, Locker J, Cassera MB, Belbin TJ, Merino EF, Dong X, Hemeon I, Evans GB, Guha C, Schramm VL. Growth and metastases of human lung cancer are inhibited in mouse xenografts by a transition state analogue of 5'-methylthioadenosine phosphorylase. *J. Biol. Chem.* 2011; 286:4902–4911. [PubMed: 21135097]
5. Basu I, Cordovano G, Das I, Belbin TJ, Guha C, Schramm VL. A Transition state analogue of 5'-methylthioadenosine phosphorylase induces apoptosis in head and neck cancers. *J. Biol. Chem.* 2007; 282:21477–21486. [PubMed: 17548352]
6. Camacho-Vanegas O, Camacho SC, Till J, Miranda-Lorenzo I, Terzo E, Ramirez MC, Schramm V, Cordovano G, Watts G, Mehta S, Kimonis V, Hoch B, Philibert KD, Raabe CA, Bishop DF, Glucksman MJ, Martignetti JA. Primate genome gain and loss: a bone dysplasia, muscular dystrophy, and bone cancer syndrome resulting from mutated retroviral-derived MTAP transcripts. *Am J Hum Genet.* 2012; 90:614–627. [PubMed: 22464254]
7. Singh V, Schramm VL. Transition-State Structure of Human 5'-Methylthioadenosine Phosphorylase. *J. Am. Chem. Soc.* 2006; 128:14691–14696. [PubMed: 17090056]
8. Singh V, Shi W, Evans GB, Tyler PC, Furneaux RH, Almo SC, Schramm VL. Picomolar Transition State Analogue Inhibitors of Human 5'-Methylthioadenosine Phosphorylase and X-ray Structure with MT-Immucillin-A. *Biochemistry.* 2004; 43:9–18. [PubMed: 14705926]
9. Evans GB, Furneaux RH, Schramm VL, Singh V, Tyler PC. Targeting the Polyamine Pathway with Transition-State Analogue Inhibitors of 5'-Methylthioadenosine Phosphorylase. *J. Med. Chem.* 2004; 47:3275–3281. [PubMed: 15163207]
10. Evans GB, Furneaux RH, Lenz DH, Painter GF, Schramm VL, Singh V, Tyler PC. Second Generation Transition State Analogue Inhibitors of Human 5'-Methylthioadenosine Phosphorylase. *J. Med. Chem.* 2005; 48:4679–4689. [PubMed: 16000004]
11. Guan R, Ho MC, Brenowitz M, Tyler PC, Evans GB, Almo SC, Schramm VL. Entropy-driven binding of picomolar transition state analogue inhibitors to human 5'-methylthioadenosine phosphorylase. *Biochemistry.* 2011; 50:10408–10417. [PubMed: 21985704]
12. Appleby TC, Erion MD, Ealick SE. The structure of human 5'-deoxy-5'-methylthioadenosine phosphorylase at 1.7 angstrom resolution provides insights into substrate binding and catalysis. *Structure.* 1999; 7:629–641. [PubMed: 10404592]
13. Edwards AA, Mason JM, Clinch K, Tyler PC, Evans GB, Schramm VL. Altered Enthalpy-Entropy Compensation in Picomolar Transition State Analogues of Human Purine Nucleoside Phosphorylase. *Biochemistry.* 2009; 48:5226–5238. [PubMed: 19425594]
14. Miles RW, Tyler PC, Furneaux RH, Bagdassarian CK, Schramm VL. One-third-the-sites transition-state inhibitors for purine nucleoside phosphorylase. *Biochemistry.* 1998; 37:8615–3621. [PubMed: 9628722]
15. Gomez J, Freire E. Thermodynamic mapping of the inhibitor site of the aspartic protease endothiapepsin. *J. Mol. Biol.* 1995; 252:337–350. [PubMed: 7563055]
16. Niesen FH, Berglund H, Vedadi M. The use of differential scanning fluorimetry to detect ligand interactions that promote protein stability. *Nature protocols.* 2007; 2:2212–2221.

Dissociative S<sub>N</sub>1 Transition State**Figure 1.**

(A) Transition state of *MTAP*. (B) Transition state analogue inhibitors of *MTAP*. The 9-deazaadenine group increases the  $pK_a$  of N7 (blue). MT-ImmA and MT-DADMe-ImmA are first and second generations of transition state analogues, respectively. pClPhT-DADMe-ImmA is a 10 pM inhibitor of *MTAP*. Transition state features and their mimics in transition state analogues are in blue.

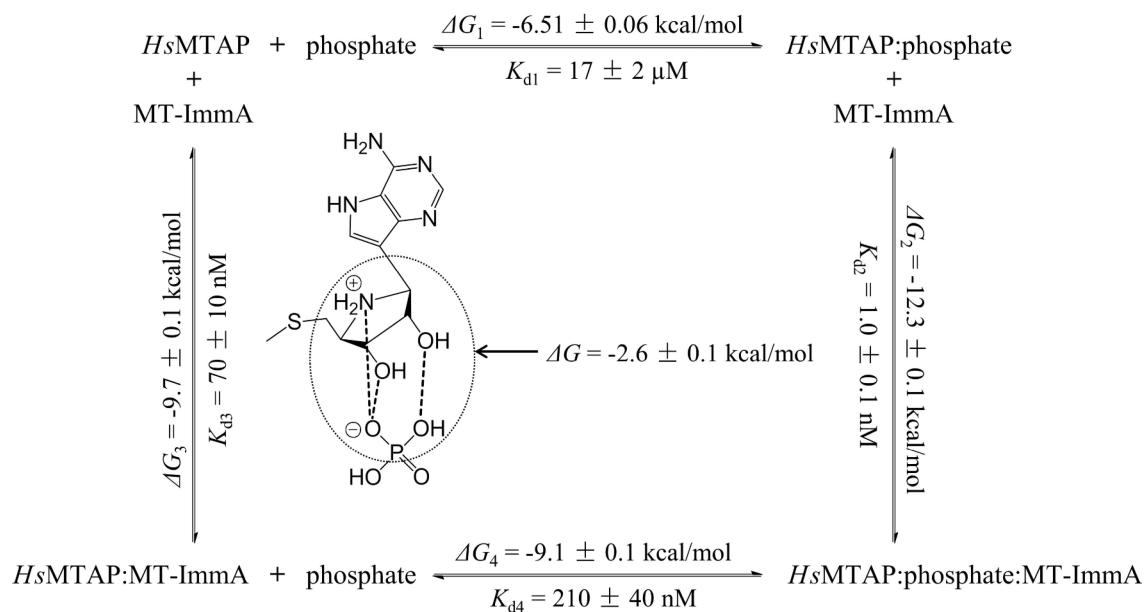


**Figure 2.**  
Isothermal titrations of apo *MTAP* with ligands in Hepes Buffer.

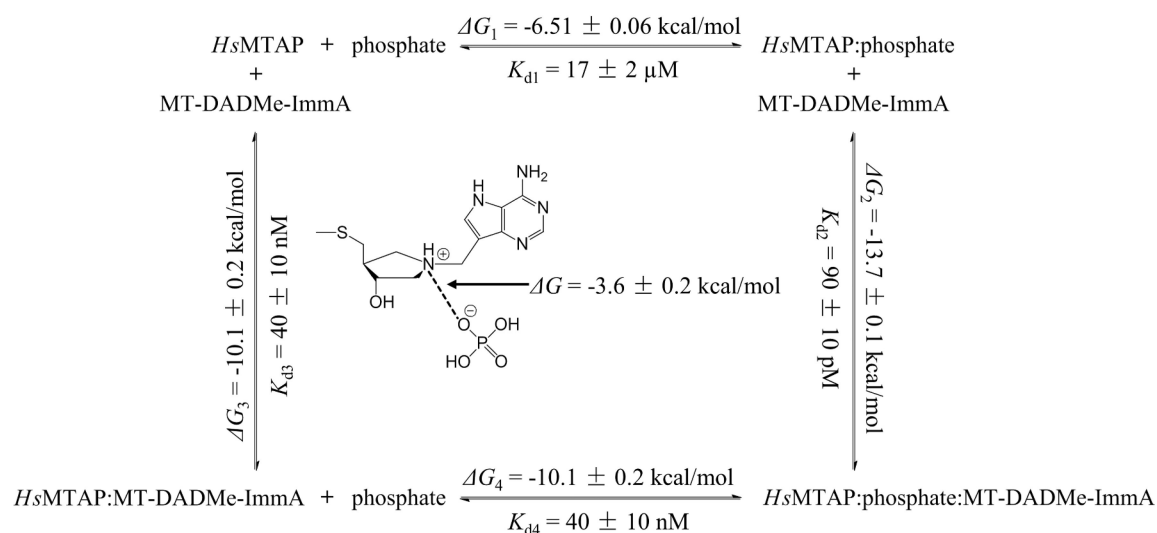


**Figure 3.**  
Isothermal titrations of apo *MTAP* with ligands in Tris Buffer.

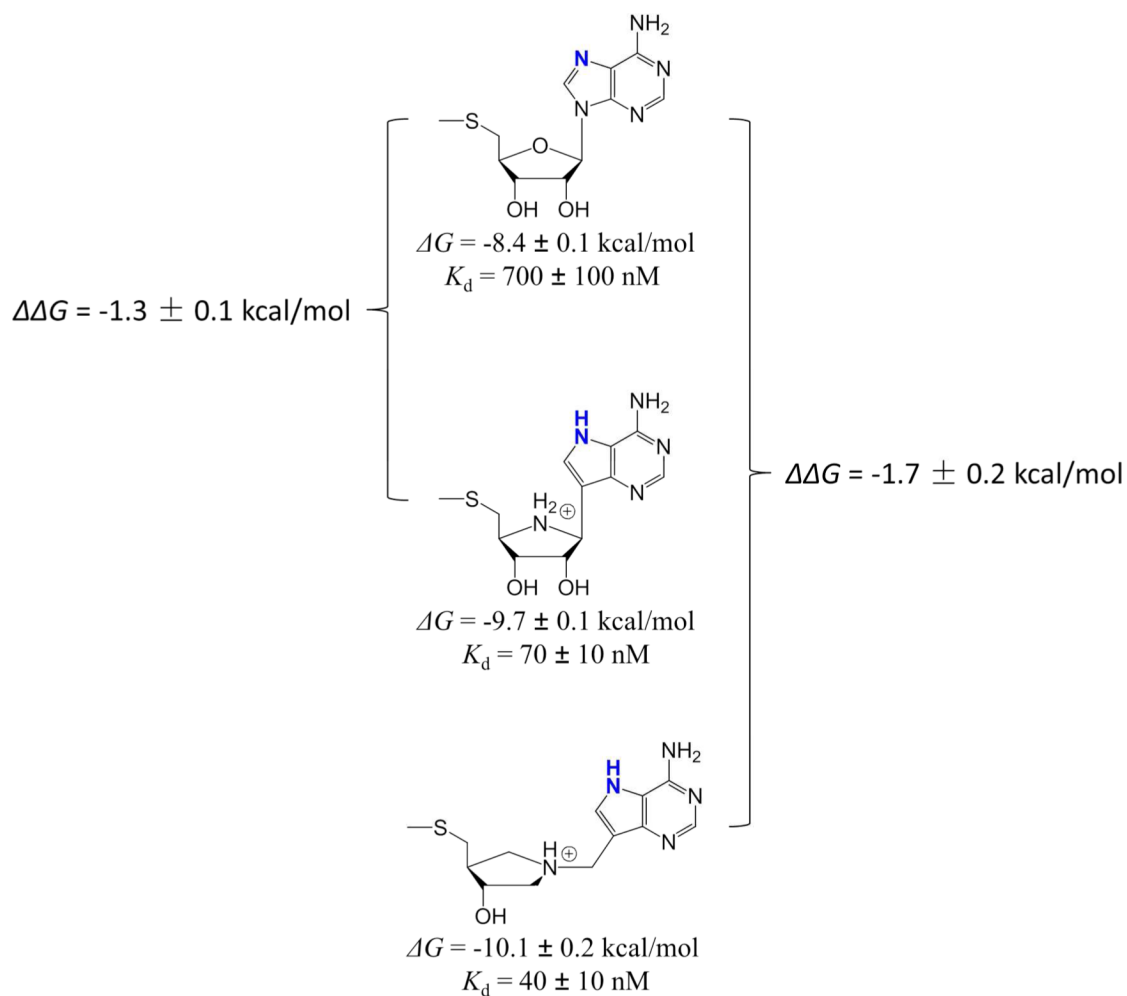


**Figure 4.**

Thermodynamic cycle of MT-ImmA and phosphate binding to *MTAP*. MT-ImmA is a first generation transition state analogue inhibitor of *MTAP*. The  $\Delta G$  and  $K_d$  values of MT-ImmA binding to *MTAP*:phosphate complex are from ref. (11). The Interaction between MT-ImmA and phosphate is indicated as dashed lines.

**Figure 5.**

Thermodynamic cycle of MT-DADMe-ImmA and phosphate binding to *MTAP*. MT-DADMe-ImmA represents the second generation transition state analogue inhibitors of *MTAP*. The  $\Delta G$  and  $K_d$  values of MT-DADMe-ImmA binding to *MTAP*:phosphate complex are from ref. (11). The Interactions between MT-DADMe-ImmA and phosphate are indicated as dashed lines.

**Figure 6.**

Thermodynamic contributions from the protonated N7 of transition state analogue inhibitors. The  $\Delta G$  and  $K_d$  values are for the binding of ligands to apo *MTAP*. The  $\Delta\Delta G$  values are calculated by subtracting the  $\Delta G$  of MTA from those of inhibitors, representing the thermodynamic contributions of protonated N7. The protonation states of N7 are colored in blue.

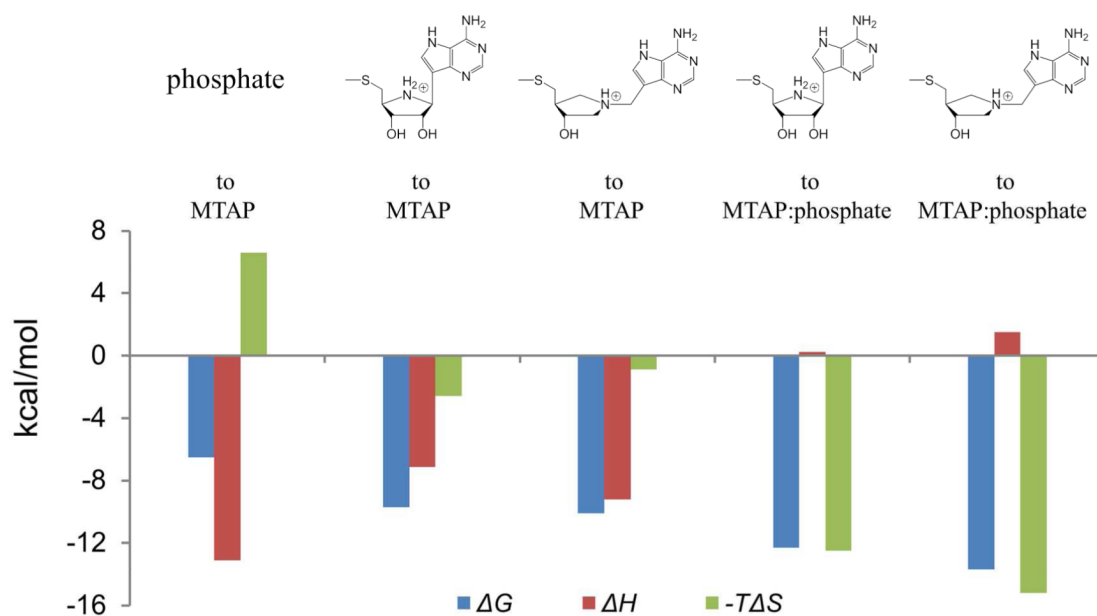


**Figure 7.** Thermodynamics signatures of ligands binding to *MTAP* and *MTAP*:phosphate complex. The thermodynamic parameters of inhibitors binding to *MTAP*:phosphate complex are from ref (11).

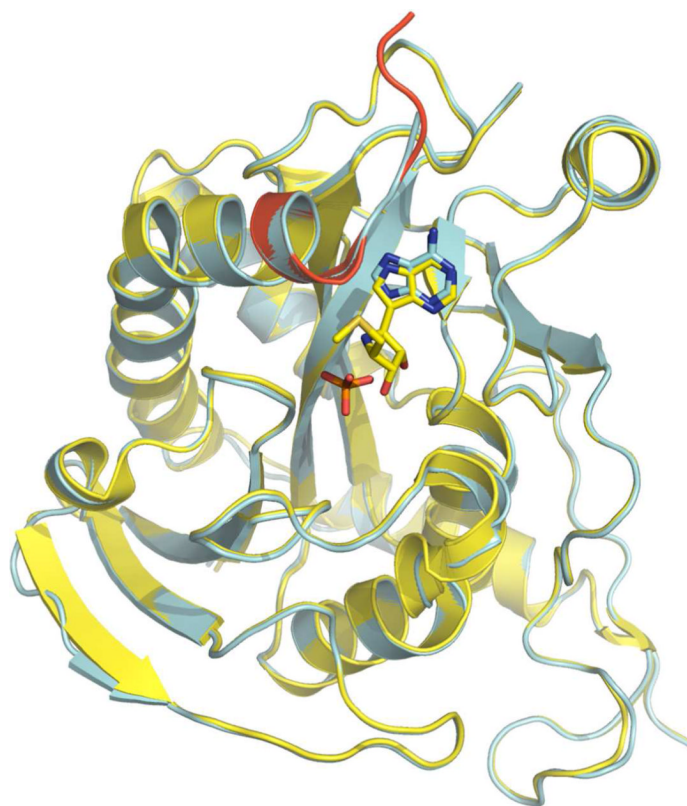


**Figure 8.**

Superimposed structures of *MTAP* in complex with adenine (PDB ID: 1CB0) and in complex with phosphate and MT-Imma (PDB ID: 1K27). 1CB0 and 1K27 are colored in cyan and yellow, respectively. The ligands are shown as sticks. The loop composed of residues 227 to 235 is responsible for the closure of the active site upon transition state analogues binding to *MTAP*:phosphate complex and is colored in red. This loop is flexible in the crystal structure of apo *MTAP* but fully ordered in the structure of *MTAP* in complex with phosphate and pClPhT-DADMe-Imma, a 10 pM second generation transition state analogue. The residues 227 to 229 of the loop are not ordered in 1CB0, while in 1K27, only the residue 227 is mobile.



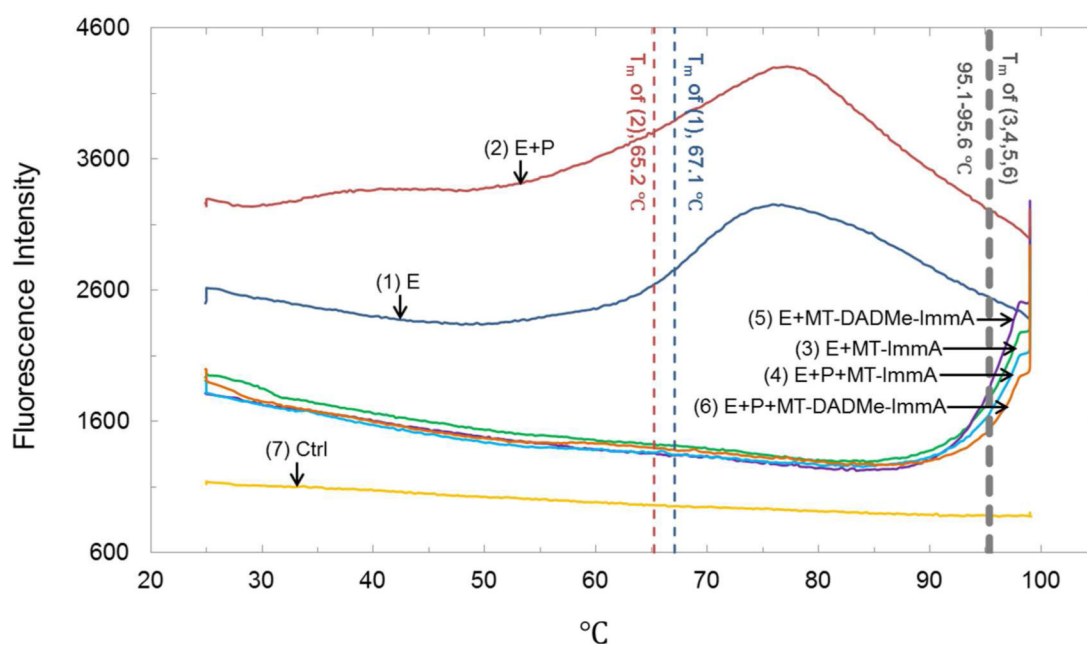


**Figure 9.**

Differential temperature scanning fluorimetry of *MTAP*. P represents 20 mM phosphate.  $T_m$  values (°C) are  $67.07 \pm 0.08$  (1),  $65.23 \pm 0.08$  (2),  $95.09 \pm 0.07$  (3),  $95.10 \pm 0.08$  (4),  $95.14 \pm 0.06$  (5), and  $95.61 \pm 0.07$  (6), respectively. Other conditions are summarized in the methods.

**Table 1**

Thermodynamic parameters for ligands binding to apo *MTAP* in Hepes buffer.

Ligand	$K_d [n]^a$ (nM)	$\Delta G$ (kcal/mol)	$\Delta H_{\text{Hepes}}$ (kcal/mol)	$-T\Delta S_{\text{Hepes}}$ (kcal/mol)
MT-ImmA	$70 \pm 10$ [3]	$-9.7 \pm 0.1$	$-9.59 \pm 0.08$	$-0.1 \pm 0.1$
MT-DADMe-ImmA	$40 \pm 10$ [2] $110 \pm 20$ [1]	$-10.1 \pm 0.2$ $-9.5 \pm 0.1$	$-10.2 \pm 0.8$ $-3 \pm 1$	$0.1 \pm 0.8$ $-7 \pm 1$
phosphate	$17000 \pm 2000$ [3]	$-6.51 \pm 0.06$	$-8.7 \pm 0.3$	$2.2 \pm 0.3$
MTA	$8 \pm 5$ [1] $700 \pm 100$ [2]	$-11.1 \pm 0.4$ $-8.4 \pm 0.1$	$-1.0 \pm 0.3$ $-6.1 \pm 0.2$	$-10.1 \pm 0.5$ $-2.3 \pm 0.2$

<sup>a</sup>  
 $n$  is the number of sites.

**Table 2**Protonation/deprotonation effects on thermodynamic parameters of ligands binding to apo *MTAP*.

Ligand	$\Delta H_{\text{Tris}} [n]^a$ (kcal/mol)	$-T\Delta S_{\text{Tris}}$ (kcal/mol)	$\Delta H_{\text{Tris}} - \Delta H_{\text{Hepes}}$ (kcal/mol)	Number <sub>Proton</sub> <sup>b</sup>	$\Delta H_{\text{correction}}^c$ (kcal/mol)	$-T\Delta S_{\text{correction}}^c$ (kcal/mol)
MT-ImmA	$-12.82 \pm 0.05$ [3]	$3.1 \pm 0.1$	$-3.23 \pm 0.09$	$0.50 \pm 0.01$	$-7.15 \pm 0.09$	$-2.6 \pm 0.1$
MT-DADMe-ImmA	$-11.4 \pm 0.2$ [2] $-10.3 \pm 0.4$ [1]	$1.3 \pm 0.3$ $0.8 \pm 0.4$	$-1.2 \pm 0.8$ $-7 \pm 1$	$0.2 \pm 0.1$ $1.1 \pm 0.2$	$-9.2 \pm 0.9$ $2 \pm 1$	$-0.9 \pm 0.9$ $-12 \pm 1$
phosphate	$-2.77 \pm 0.04$ [3]	$-3.74 \pm 0.07$	$5.9 \pm 0.3$	$-0.91 \pm 0.05$	$-13.1 \pm 0.4$	$6.6 \pm 0.4$

<sup>a</sup>  $n$  is the number of sites.<sup>b</sup> Number of protons released from the binding of ligand to *MTAP*. The ionization enthalpy of Hepes and Tris buffers are 4.876 and 11.341 kcal/mol, respectively (16). The enthalpy change of  $\Delta H_{\text{Tris}} - \Delta H_{\text{Hepes}}$  is  $-6.465$  kcal/mol for each proton released from the binding complex.<sup>c</sup>  $\Delta H_{\text{correction}}$  and  $-T\Delta S_{\text{correction}}$  represent the  $\Delta H$  and  $-T\Delta S$  without any effects from the protonation or deprotonation during the binding.